EVOLUTION OF SPACECRAFT ORBITAL MOTION DUE TO HYPERVELOCITY IMPACTS WITH DEBRIS AND METEOROIDS

Luc Sagnières and Inna Sharf

Department of Mechanical Engineering, McGill University, 817 Sherbrooke W., Montreal, QC, H3A 0C3, Canada, Email: luc.sagnieres@mail.mcgill.ca

ABSTRACT

A framework is developed to include the effect of bombardment from space debris and meteoroids on the orbital motion of active and inoperative satellites by considering the transfer of momentum from impactors as a stochastic process known as a compound Poisson process. The differential equation for orbital motion is set up as a stochastic differential equation and solved in a Monte Carlo simulation. The orbital propagation is coupled to a deterministic attitude propagation model in order to implement the additional effect of ejecta momentum. The framework is applied to four spacecraft and two analytical test cases are presented in order to obtain a confirmation of the validity of the stochastic model. The resulting probability distribution functions for the change in semi-major axis after a ten-year propagation period show that for the presented cases, a systematic decrease is present, although small compared to observations and estimated decay due to other effects.

Key words: hypervelocity impacts, orbit propagation, stochastic differential equation.

1. INTRODUCTION

Collisions between small orbital debris and micrometeoroids and active and inoperative satellites are typically considered in the context of the increasing threat that they present to space operations and missions [8]. The current estimates of the space debris population in orbit are 29,000 above 10 cm, 670,000 above 1 cm, and more than 170 million above 1 mm [4]. Furthermore, every day approximately 100 tons of dust and sand-sized meteoroids enter Earth's atmosphere [9]. When colliding with orbiting spacecraft, these hypervelocity impacts, occurring at speeds up to 60 km per second, can have disastrous consequences because of the structural damage they may cause and electromagnetic interference they may have with spacecraft systems [3]. When impacting large debris, this bombardment is responsible for generating more small debris in orbit, further aggravating the space debris problem.

From a somewhat different perspective, the impacts between the small debris flux and a large object, be it a functional or defunct spacecraft, will lead to a transfer of momentum from the impactor to the target, thus modifying its orbital parameters. Moreover, at such high velocities, the particles ejected during crater formation provide an additional momentum transfer, an effect known as momentum enhancement [12]. While many of the environmental factors influencing an object's orbit in space have been extensively studied, the effect of bombardment of debris and meteoroids on spacecraft orbit propagation, on the other hand, is a research area that is still in its infancy. The work proposed here follows the methodology described in [14] for propagating the attitude motion of tumbling spacecraft undergoing these hypervelocity impacts, however, applying that approach to orbital motion.

This method enables the inclusion of hypervelocity impacts into spacecraft orbit propagation models by considering the transfer of linear momentum from collisions as a stochastic jump process known as a compound Poisson process [14]. The differential equation for orbital motion then becomes a stochastic differential equation (SDE) and is solved in a Monte Carlo simulation by employing independent sets of randomly generated collisions [14]. These collisions can be obtained using impact fluxes converted into probability density functions (PDF), the former obtained from the European Space Agency's (ESA) Meteoroid and Space Debris Terrestrial Environment Reference (MASTER) model describing the debris and meteoroid population around Earth [5]. Furthermore, the stochastic orbit propagation model can be coupled to a deterministic attitude propagation model in order to adequately implement the additional effect of ejecta momentum which is dependent on the orientation of the spacecraft. The momentum contribution from ejecta can be calculated for every collision by considering the velocity, mass and direction distribution of the ejecting particles from a model developed for ESA defining the characteristics of such ejecta [12].

First, a review of the differential equations governing spacecraft dynamics will be presented in Section 2. Second, the SDEs for orbital motion will be discussed in Section 3 along with the numerical integration method used to solve them. In order to assess the importance of these collisions on orbit propagation, the developed

model is then applied to several pieces of orbital objects in Section 4: the defunct European environmental satellite Envisat, representing a potential active debris removal (ADR) target in low-Earth orbit (LEO); a high area-to-mass ratio (HAMR) object modeled after multi-layer insulation debris in a highly elliptic orbit with apogee at geostationary altitude, chosen to represent an upper bound when the effect of the collisions is strongest; one of the operational LAGEOS spherical satellites in a medium Earth orbit (MEO), satellites having been the cause of some debate due to unexplained semi-major axis decay; and lastly to the Japenese satellite Ajisai, also an operational spherical satellite undergoing an orbital decay due to aerodynamic drag. Finally, in Section 5, two analytical test cases are presented to provide additional confidence in the validity of the propagation model.

2. SPACECRAFT DYNAMICS

Understanding the dynamics of satellites in orbit requires analysis of the six degrees of freedom governing the orbit and attitude of the spacecraft: three for translation and three for orientation. Three vector differential equations describe the evolution of the corresponding variables. First is the dynamics equation for orbital motion in an Earth-centered inertial (ECI) coordinate frame [2]:

$$\ddot{\mathbf{r}}(t) = -\frac{\mu}{r(t)^3}\mathbf{r}(t) + \sum_j \mathbf{a}_j(t, \mathbf{r}(t)) \tag{1}$$

where $\mathbf{r}$ is the position as a function of time t, $r = \|\mathbf{r}\|$, μ is the Earth's gravitational parameter, and $\mathbf{a}_i$ represents the non-gravitational accelerations, and assuming a perfectly uniform spherical Earth, ignoring Earth's oblateness and third-body interactions.

The second differential equation, the dynamics equation for attitude motion, relates the evolution of angular velocity, $\boldsymbol{\omega}$, to the sum of the external torques about the center of mass of the body, $\boldsymbol{\tau}_j$ [6]:

$$\mathbf{I}\dot{\boldsymbol{\omega}}(t) + \boldsymbol{\omega}(t)^{\times}\mathbf{I}\boldsymbol{\omega}(t) = \sum_j \boldsymbol{\tau}_j(t, \mathbf{q}(t)) \tag{2}$$

where $\mathbf{I}$ is the matrix representation of the inertia tensor of the rigid body in the centroidal body-fixed frame and $\mathbf{q} = \begin{bmatrix} q_0 & \mathbf{q}_v^T \end{bmatrix}^T$ is the attitude parametrization, chosen here to be quaternions.

Finally, the third differential equation is the kinematic equation for orientation:

$$\dot{\mathbf{q}}(t) = \frac{1}{2}\boldsymbol{\Omega}(\omega)\mathbf{q}(t) \tag{3}$$

where, expressed in terms of the body-referenced components of $\boldsymbol{\omega}$:

$$\boldsymbol{\Omega} = \begin{bmatrix} 0 & -\omega_x & -\omega_y & -\omega_z \\ \omega_x & 0 & \omega_z & -\omega_y \\ \omega_y & -\omega_z & 0 & \omega_x \\ \omega_z & \omega_y & -\omega_x & 0 \end{bmatrix} \tag{4}$$

3. INCLUDING HYPERVELOCITY IMPACTS IN ORBITAL MOTION

As hypervelocity impacts are random, they will have to be considered as a stochastic process and the differential equation for orbital motion will have to be set up as an SDE. A stochastic process is one that describes the evolution of a system's random variables over time, and, unlike deterministic processes, can expand in multiple, or infinitely many, paths [11]. Including stochastic processes in differential equations is useful when wanting to describe uncertainties or random variations in any dynamical system. Solving SDEs requires the use of numerical integration techniques that have been a subject of interest in the last few decades as most integration methods used for solving ordinary differential equations perform poorly when applied to SDEs [11].

3.1. Collisions as a compound Poisson process

As explained in [14], the momentum transfer due to hypervelocity impacts can be represented as a compound Poisson process if a PDF describing the impacts can be determined, and if the time between collisions can be shown to follow an exponential distribution. PDFs for the mass and velocity of the impactors can be obtained by transforming the velocity and mass impact fluxes of the MASTER-2009 model for a certain input orbit. A 2D PDF for direction can also be obtained in an analogous manner from the directional impact flux as a function of azimuth and elevation angles. These PDFs can then be combined to define the linear momentum of an impactor.

The time between collisions can be assumed to follow an exponential distribution due to the analogy between kinetic gas theory and objects sweeping the space environment filled with other debris and meteoroids [5]. Therefore, the PDF for time between collisions can be obtained from the total expected number of collisions as outputted by MASTER-2009. The four PDFs obtained then define the impactors that a spacecraft in the specified orbit will collide with.

From Eq. (1), the differential equation of motion can be set up in differential form:

$$d\dot{\mathbf{r}}(t) = \left(-\frac{\mu}{r(t)^3}\mathbf{r}(t) + \sum_j \mathbf{a}_j(t, \mathbf{r}(t)) \right) dt \tag{5}$$

Considering the momentum of the satellite, defined as $\mathbf{p} = M\dot{\mathbf{r}}$ with M the mass of the spacecraft, Eq. (5) can be rewritten as:

$$d\mathbf{p}(t) = M \left(-\frac{\mu}{r(t)^3}\mathbf{r}(t) + \sum_j \mathbf{a}_j(t, \mathbf{r}(t)) \right) dt \tag{6}$$

Including the term for the momentum from hypervelocity impacts as a function of the compound Poisson process,

$\mathbf{Y}_t$, Eq. (6) is transformed into an SDE:

$$d\mathbf{p}(t) = M\left(-\frac{\mu}{r(t)^3}\mathbf{r}(t) + \sum_j \mathbf{a}_j(t, \mathbf{r}(t))\right)dt + d\mathbf{Y}_t \tag{7}$$

As shown in [14], hypervelocity impacts have a minimal effect on the evolution of angular velocity and a deterministic approach to attitude propagation can therefore be applied. Therefore, Eq. (7), along with Eqs. (2) and (3) define the dynamics of any satellite orbiting Earth undergoing bombardment of debris and meteoroids.

3.2. Solving the stochastic differential equation

The numerical integration method used to solve the stochastic jump process in Eq. (7) requires a jump-adapted time discretization method, where the time discretization is constructed to include the jump times on top of the regular time steps [11]. Once the jump times are known, generated randomly by the method presented in [14], solving Eq. (7) then reduces to: first using any numerical integration method to propagate the position vector without considering collisions, *i.e.*, integrating forward the following first-order ODE:

$$\frac{d\mathbf{p}(t)}{dt} = M\left(-\frac{\mu}{r(t)^3}\mathbf{r}(t) + \sum_j \mathbf{a}_j(t, \mathbf{r}(t))\right) \tag{8}$$

Second, if time step t_{n+1} is a jump time, the estimate of momentum obtained from Eq. (8) at the next time step, $\mathbf{p}_{t_{n+1}}^-$, is updated using the following jump condition:

$$\mathbf{p}_{t_{n+1}} = \mathbf{p}_{t_{n+1}}^- + \Delta\mathbf{Y}_{t_{n+1}} \tag{9}$$

where $\Delta\mathbf{Y}_{t_{n+1}} = \mathbf{Y}_{t_{n+1}} - \mathbf{Y}_{t_{n+1}^-}$ is the jump size of the compound Poisson process at jump time t_{n+1}, describing the relative linear momentum of the impactor, and calculated as shown below. Derivation of the jump condition and the reason for the use of relative linear momentum, in contrast to absolute linear momentum, can be found in Sections 3.3 and 3.4.

3.3. Generating independent collisions

Following the methodology outlined in [14], one can obtain random values for impactor mass m, relative impact velocity v_{rel}, elevation angle θ, and azimuth ϕ from the obtained PDFs using inverse transform sampling. A vector for the relative impactor velocity in the orbital reference frame can then be computed by switching from spherical coordinates to Cartesian coordinates (x in the spacecraft ram direction; z pointing towards Earth; y completing the right hand rule) using:

$$\mathbf{v}_{\text{rel}}^O = \begin{bmatrix} -v_{\text{rel}}\ \cos\theta\ \cos\phi \\ -v_{\text{rel}}\ \cos\theta\ \sin\phi \\ v_{\text{rel}}\ \sin\theta \end{bmatrix} \tag{10}$$

Knowing the position and velocity of the satellite in its orbit at the current time step, the relative velocity in the inertial frame, $\mathbf{v}_{\text{rel}}$, can be obtained from the associated rotation matrix, $\mathbf{C}_{IO}(t)$:

$$\mathbf{v}_{\text{rel}} = \mathbf{C}_{IO}(t_{n+1})\mathbf{v}_{\text{rel}}^O \tag{11}$$

From this, the relative momentum vector of the impactor in the inertial frame can be determined, and used in Eq. (9):

$$\Delta\mathbf{Y}_{t_{n+1}} = m\mathbf{v}_{\text{rel}} \tag{12}$$

3.4. Momentum exchange and the jump condition

The derivation of Eq. (9) starts by looking at the momentum exchange between the impactor and the target at the moment of impact t_{n+1} in the inertial frame, where the subscript i here represents the impactor, and the superscript $()^-$ represents the time right before the impact. Thus, using conservation of momentum over the duration of impact, we have:

$$\Delta\mathbf{p}_{t_{n+1}} = -\Delta\mathbf{p}_{i,t_{n+1}} \tag{13}$$

or equivalently:

$$\mathbf{p}_{t_{n+1}} = \mathbf{p}_{t_{n+1}}^- + \mathbf{p}_{i,t_{n+1}}^- - \mathbf{p}_{i,t_{n+1}} \tag{14}$$

In terms of velocity, where M is the mass of the target and m is the mass of the impactor:

$$M\mathbf{v}_{t_{n+1}} = M\mathbf{v}_{t_{n+1}}^- + m\mathbf{v}_{i,t_{n+1}}^- - m\mathbf{v}_{i,t_{n+1}} \tag{15}$$

The velocities after impact are equal, assuming the impactor is absorbed by the target:

$$M\mathbf{v}_{t_{n+1}} = M\mathbf{v}_{t_{n+1}}^- + m\mathbf{v}_{i,t_{n+1}}^- - m\mathbf{v}_{t_{n+1}} \tag{16}$$

The velocity of the impactor right before impact can be written in terms of the velocity of the target and the relative velocity of the impactor:

$$\mathbf{v}_{i,t_{n+1}}^- = \mathbf{v}_{t_{n+1}}^- + \mathbf{v}_{\text{rel}} \tag{17}$$

Therefore:

$$M\mathbf{v}_{t_{n+1}} = M\mathbf{v}_{t_{n+1}}^- + m\mathbf{v}_{t_{n+1}}^- + m\mathbf{v}_{\text{rel}} - m\mathbf{v}_{t_{n+1}} \tag{18}$$

and solving for $\mathbf{v}_{t_{n+1}}$:

$$(M+m)\mathbf{v}_{t_{n+1}} = (M+m)\mathbf{v}_{t_{n+1}}^- + m\mathbf{v}_{\text{rel}} \tag{19}$$

Simplifying for $M \gg m$ gives:

$$M\mathbf{v}_{t_{n+1}} = M\mathbf{v}_{t_{n+1}}^- + m\mathbf{v}_{\text{rel}} \tag{20}$$

or in terms of momentum:

$$\mathbf{p}_{t_{n+1}} = \mathbf{p}_{t_{n+1}}^- + m\mathbf{v}_{\text{rel}} \tag{21}$$

This is the jump condition used for propagating the momentum of the target during a collision as seen in Eq. (9) coupled with Eq. (12).

3.5. Ejecta Momentum and Coupling to Attitude Propagation

As an impactor collides with the target, a large amount of particulates in the vicinity of the location of impact brakes off from the target's surface and is ejected outwards [12]. These particles have an associated momentum and therefore increase the effect of the momentum transfer from the impactor to the target. A model was developed primarily for ESA to describe the ejecta population that is created during such a hypervelocity impact [12]. It postulates that three ejection processes occur: small particles thrown off at grazing angles and high velocities, known as jetting; cone fragments, which are small and fast particles that are ejected at a constant elevation angle in a cone around the location of impact; and spall products, large fragments ejected normal to the impact surface at low velocities [12]. This model describes the velocity, size, and direction distributions for each ejection process as a function of the impactor's characteristics and from these, a vector for the linear momentum contribution of the ejecta can be calculated [14].

Implementing this effect in the orbit propagation of large space debris requires knowledge of the target's orientation at the moment of impact. Therefore, the attitude of the target needs to be propagated in parallel. The equations for rotational motion and translational motion can be propagated separately and the coupling is only performed at the times of impact when information about attitude is used in the calculation of the momentum contribution from ejecta.

4. CASE STUDIES

To understand the influence of hypervelocity impacts on orbital motion, the differential equations of motion were propagated for ten years considering only hypervelocity impacts and the Earth's gravitational force. The method was applied to four cases, Envisat, a HAMR object, LAGEOS and Ajisai, and each ten-year run was repeated 10,000 times for different randomly generated sets of collisions including the effect of ejecta momentum. A solution without momentum enhancement was also computed for Envisat in order to compare with our analytical test case in Section 5. As Envisat can be considered to be spin-stabilized, a constant spin rate is assumed and external torques can therefore be neglected. The HAMR object is randomly tumbling, so excluding external torques will also not provide a bias in the results. Finally, LAGEOS and Ajisai are spherical satellites and the changes in attitude are not important. The impact fluxes used are assumed to be constant throughout the propagation. The flowchart outlining the complete methodology is presented in Fig. 1. The inputs include the orbital parameters and the initial conditions of the differential equations. The output includes the probability distributions for the orbital parameters. The fraction of the algorithm which is in the Monte Carlo simulation is delineated with a box.

4.1. Envisat

Envisat was a European Earth-observing environmental satellite launched by ESA on March 1, 2002. It was sent in a Sun synchronous polar orbit at an altitude of 790 km. The purpose of the satellite was to monitor climate change and the Earth's environmental resources. The expected mission lifetime was 5 years but it lasted until April 8, 2012, when ESA lost contact with the satellite for unknown causes, and then announced its end of mission on May 9, 2012. To this day, Envisat remains in orbit and is one of the largest space debris objects currently being tracked by the United States Space Surveillance Network (SSN). Due to its large size and busy polar orbit, Envisat has been of much interest to the community as a potential ADR target.

Envisat is assumed to be spinning at a rate of 2.67° s^{-1} and weighs approximately 7828 kg with a total surface area of 332 m^2 [7, 1]. The orbit parameters used are a semi-major axis (SMA) of 7136 km, an eccentricity of 0.0001 and an inclination of 98.3°. Using its total surface area and current orbit as input to MASTER-2009, a total of 5.77×10^5 impacts per year, or about one per minute, can be expected, with 58% coming from micrometeoroids. Figs. 2a and 2b show the PDFs for the change in SMA throughout the ten-year simulations for the case with and without momentum enhancement, where a yearly orbital decay of 0.96 m and 0.74 m are seen, respectively. Furthermore, the widths of the PDFs increase with time, as expected, and are larger for the case with momentum enhancement, similarly to what was obtained in [14] for attitude motion. However, for such a large spacecraft at a relatively low orbit, aerodynamic drag will have a much larger influence on the orbital decay of the satellite, calculated to be up to 2 km per year depending on solar activity. Similar PDFs were obtained for the orbit eccentricity, inclination, right ascension of the ascending node and argument of perigee, but changes in them are minute and deemed negligible.

4.2. High Area-to-Mass Ratio Object

The same procedure was repeated using the properties of a HAMR object. A flat two-sided 1×1 m^2 plate with a mass of 0.1 kg was employed, therefore having an area-to-mass ratio of 20, simulating a piece of MLI debris [15]. An initial angular velocity of $\omega_0 = [1, 1, 1]^T$ $^\circ$ s^{-1} was used to simulate tumbling. The orbit used to calculate the impact fluxes from MASTER-2009 has a SMA of 24,802 km, an eccentricity of 0.7, and an inclination of 15° [15]. The total number of expected collisions for that orbit was found to be close to 870 per year per m^2, with about 93% coming from meteoroids. 1739 collisions are therefore expected to occur per year, or one every 5 hours.

For such an object, the effect of hypervelocity impacts will be much greater, similarly to what was seen in [14]. Indeed, Fig. 3 shows distributions with much larger

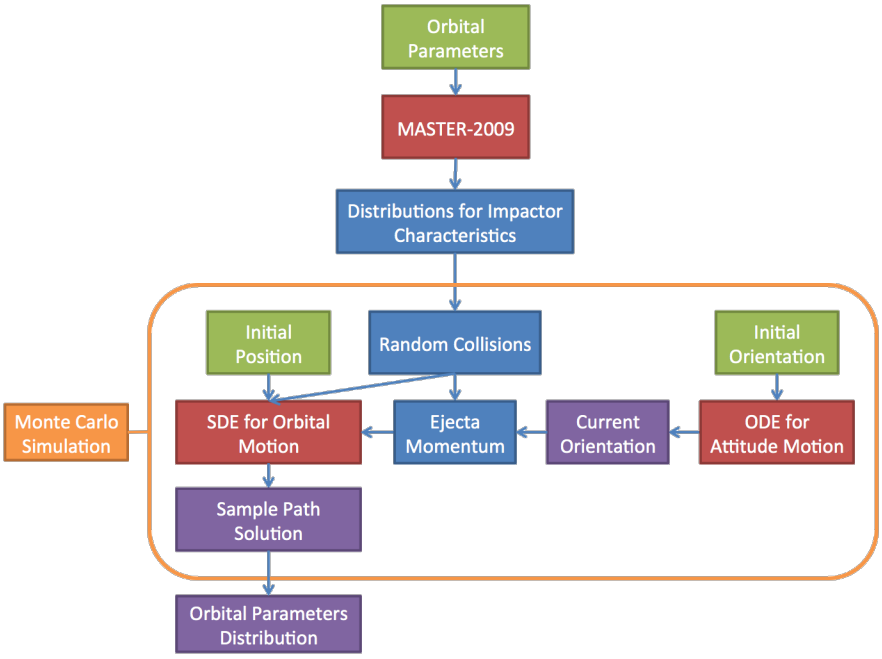

Figure 1. Flowchart of the Algorithm for Coupled Orbit-Attitude Propagation from Hypervelocity Impacts

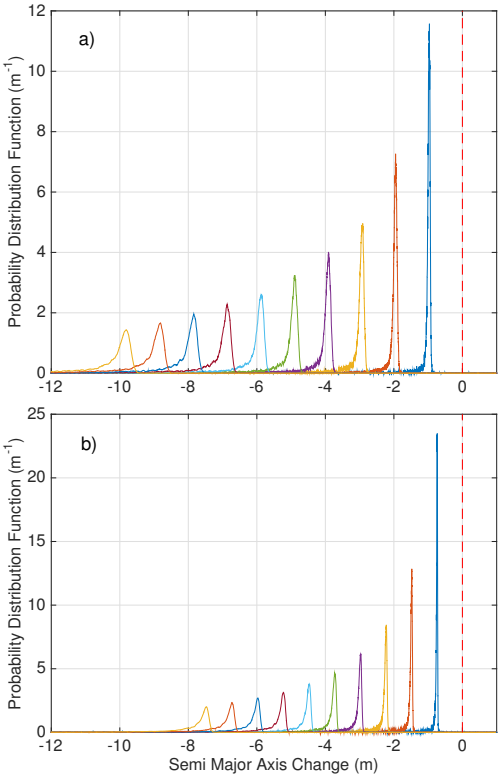

Figure 2. SMA PDF Evolution for Envisat (a) with Momentum Enhancement and (b) without

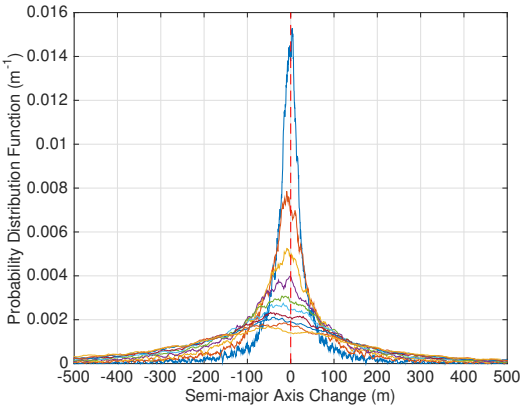

Figure 3. SMA PDF Evolution for the HAMR Object

widths (hundreds of meters compared to $<$ 1 m for Envisat), and a decrease in the distribution center of about 8 m per year. Similar large variations in the distributions of other orbital elements can also be seen. Due to the small change in SMA and the large distribution widths, a non-negligible possibility of the orbit being raised exists. The widths of the distributions are related to the spread in directionality of the impacts: the wide spread is due to the fact that most impacts in this high-altitude orbit occur with meteoroids and these come from every direction. Because impacts are not mainly coming from the ram direction, as is the case for Envisat, some of the one-year propagations end up with more collisions causing an increase in the SMA.

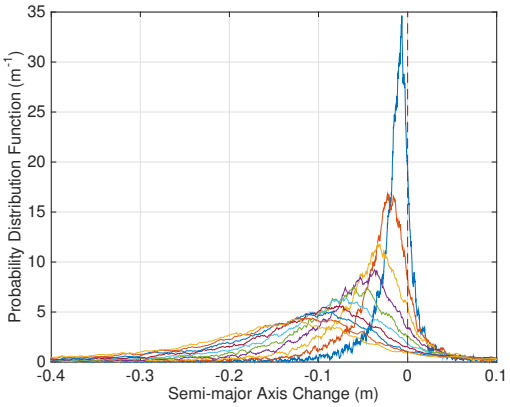

Figure 4. SMA PDF Evolution for LAGEOS

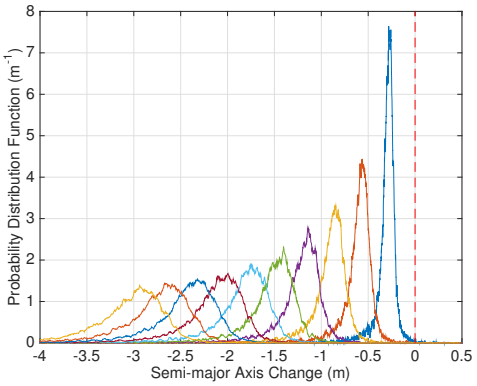

Figure 5. SMA PDF Evolution for Ajisai

4.3. LAGEOS

The LAGEOS satellites are spherical satellites used for providing a laser ranging benchmark for geodynamical studies. LAGEOS-1 is an aluminum sphere with a brass core with a radius of 30 cm orbiting at a SMA of 12274 km, an inclination of 109.9° and eccentricity of 0.0039. It was launched in 1976 and has been the cause of some debate after observations determined it experiences an orbital decay of approximately 1 mm per day [13]. Because of its high altitude, aerodynamic drag is negligible and some possible decay mechanisms include the Yarkovsky thermal drag and charged particle drag, as well as the effect of the Earth's inertial induction [13]. We attempt here to establish whether hypervelocity impacts with micrometeoroids and small debris could play a role in the observed decrease of the spacecraft altitude.

Fig. 4 shows the output of the stochastic model, with the yearly PDFs for the change in SMA. Approximately 5.1×10^3 collisions per year are expected, 90% of them from micrometeoroids. A yearly decrease in the distribution centers of approximately 8 mm is seen. This represents only about 2% of the orbital decay observations for the satellite, showing that this effect is considerably smaller than the other effects suggested above. Once again, a small probability of orbit raising exists due to the high proportion of impacts from meteoroids, thus leading to wide distributions.

4.4. Ajisai

The last case that was looked at is the Japenese satellite Ajisai launched in 1986. It is a 685 kg hollow sphere with a diameter of 2.15 m. It is in a nearly circular orbit with a SMA of 7865 km and an inclination of 50°. From the MASTER-2009 fluxes, 7.8×10^4 collisions are expected to occur every year, with 75% from meteoroids. It was reported in [10] that the satellite underwent a decay in SMA of 42.6 m and 94.6 m during three-year periods of low solar activity and high solar activity, respectively, assumed to be caused by aerodynamic drag. These values were compared to the outputs of the stochastic model in Fig. 5, which shows the evolution of the PDF for the variation in the SMA throughout a ten-year period. A decrease of approximately 29 cm per year is observed, which is less than 1% of the observed decay due to aerodynamic drag and is therefore negligible in comparison.

From the results of the four case studies performed above, a number of consistent and expected observations can be made. First, there is a widening of the PDFs with time. Second, all PDFs indicate that the orbits are much more likely to be lowered, although in the case of the HAMR object there is a non-negligible probability of the orbit being raised. This is due to the combination of a relatively small decrease in the expected SMA and wide probability distributions. The widths of the distributions seem to be related to the directionality of the impacts, and therefore the proportion of impacts coming from meteoroids: a larger percentage of meteoroid impacts leads to wider distributions. Third, all PDFs have a characteristic shape sloping more shallowly and broadly towards negative values, again giving a clear bias towards orbit lowering. Finally, when comparing to other sources of orbit perturbations, hypervelocity impacts contribute little to the observed or expected decay values.

5. ANALYTICAL TEST CASES

Additional confidence in the validity of the orbit propagation model is given from two analytical test cases: one with a hypothetical spacecraft undergoing simple collisions, and the other with Envisat and its collisions according to MASTER-2009. The validation process involves comparing two solutions for each test case: on the one hand, a simulation of bombardment of impactors leading to orbital decay; and on the other hand, a Hohmann transfer from the same initial orbit to the resulting decayed orbit obtained by two hypothetical large impacts. The validation involves comparing the total mass of the impactors in the simulation to the sum of the impactors in the equivalent analytical Hohmann transfer.

5.1. Hohmann Transfer from Hypervelocity Impacts

From its definition, a Hohmann transfer from a circular orbit at (r_A, v_A) to a lower orbit at (r_B, v_B), with:

$$v_k = \frac{\mu}{r_k}, k \in \{A, B\} \tag{22}$$

where μ is Earth's gravitational parameter, is a two-impulse maneuver using an elliptical transfer orbit with eccentricity:

$$e = \frac{r_A - r_B}{r_A + r_B} \tag{23}$$

The velocity changes to go from the outer circular orbit to the Hohmann transfer orbit, and from the Hohmann transfer orbit to the inner circular orbit, are, respectively:

$$\begin{aligned} \Delta v_A &= v_{A_H} - v_A \\ \Delta v_B &= v_B - v_{B_H} \end{aligned} \tag{24}$$

where v_{A_H} is the velocity of the spacecraft at the point that joins the outer orbit and the transfer orbit and v_{B_H} is the velocity of the spacecraft at the intersection of the inner orbit and the transfer orbit, calculated as:

$$v_{k_H} = \frac{\sqrt{(1+e) r_k \mu}}{r_k}, k \in \{A, B\} \tag{25}$$

By considering the two impulses leading to Δv_A and Δv_B as caused by collisions with large masses, m_1 and m_2, impacting at some relative velocity, v_{rel}, one can apply conservation of momentum over the two impulses as:

$$M v_A + m_1 (v_A - v_{\text{rel}}) = (M + m_1) v_{A_H} \tag{26}$$

$$M v_{B_H} + m_2 (v_{B_H} - v_{\text{rel}}) = (M + m_2) v_B \tag{27}$$

Solving for m_1 and m_2 gives:

$$m_1 = \frac{M \Delta v_A}{-\Delta v_A - v_{\text{rel}}} \tag{28}$$

$$m_2 = \frac{M \Delta v_B}{-\Delta v_B - v_{\text{rel}}} \tag{29}$$

The validation exercise is now applied to the two aforementioned test cases, by comparing the sum of m_1 and m_2 to the sum of the debris and meteoroid flux throughout the orbital propagation time-frame, between the corresponding two orbits.

5.2. Hypothetical Spacecraft

The first test case involves a $M = 100$ kg satellite in a circular orbit at an initial altitude of 1000 km. A propagation was computed constraining the general formulation in Section 3 to allow only the bombardment from head-on collisions every 60 s, with impactors having a mass of 10^{-12} kg and with an impact velocity of 15 km s^{-1}. This simulation showed a decay in the semi-major axis of 0.1582 m after one year. The sum of the impactor masses experienced during the one-year simulation is:

$$\begin{aligned} \sum_j m_j &= 365.25 \times 60 \times 24 \times 10^{-12} \\ &= 5.2596 \times 10^{-7} \text{ kg} \end{aligned} \tag{30}$$

Substituting in Eqs. (23) through (29) the corresponding values for $M = 100$ kg, $v_{\text{rel}} = 15$ km s^{-1}, $r_A = 7371$ km and $r_B = 7371 - (0.1582 \times 10^{-3})$ km, we obtain:

$$m_1 = m_2 = 2.6298 \times 10^{-7} \text{ kg} \tag{31}$$

so that:

$$m_1 + m_2 = 5.2597 \times 10^{-7} \text{ kg} \tag{32}$$

Comparing the results of Eqs. (30) and (32) gives credence to the validity of our stochastic model.

5.3. Envisat

The second, and more general, test case involves the results of the case study presented in Section 4.1. As shown in Fig. 2b, the decrease in SMA witnessed by Envisat after one year due to collisions only, without including the effect of ejecta momentum, is approximately 0.736 m. From the MASTER-2009 impact fluxes, the expected value for the impact velocity is calculated as 16.1449 km s^{-1} and the median sum of the impactor masses from each of the 10,000 runs is approximately 3.00×10^{-4} kg.

Following the same methodology as in the previous section, one can calculate the masses of the two impactors needed to perform the corresponding Hohmann transfer. In this case, $M = 7828$ kg, $v_{\text{rel}} = 16.1449$ km s^{-1}, $r_A = 7136$ km, and $r_B = 7136 - (0.736 \times 10^{-3})$ km. From Eqs. (23)-(29), the two impact masses are therefore found to be:

$$m_1 = m_2 = 9.3436 \times 10^{-5} \text{ kg} \tag{33}$$

so that:

$$m_1 + m_2 = 1.8687 \times 10^{-4} \text{ kg} \tag{34}$$

Comparing the result in Eq. (34) to the value of 3×10^{-4} kg, as predicted by the Monte Carlo simulations, shows a significant difference. This is to be expected, as the directionality of the impactors, included in the stochastic orbital propagation but not in the analytical Hohmann transfer, where the two collisions are assumed to be head-on, will produce a smaller effect in the reduction of the SMA. Indeed, from the MASTER-2009 direction flux, approximately 60% of the collisions occur with $\pm 45^\circ$ elevation and azimuth.

However, it is possible to take this directionality spread into account analytically by looking at the spacecraft's

derived PDF for direction. A reduction factor can be obtained by integrating the direction-dependent flux over the entire sphere of directions:

$$\mathbf{D} = \begin{bmatrix} -\int_{-\pi}^{\pi}\int_{-\frac{\pi}{2}}^{\frac{\pi}{2}} F(\theta,\phi)\ \cos\theta\ \cos\phi\ d\theta\ d\phi \\ -\int_{-\pi}^{\pi}\int_{-\frac{\pi}{2}}^{\frac{\pi}{2}} F(\theta,\phi)\ \cos\theta\ \sin\phi\ d\theta\ d\phi \\ -\int_{-\pi}^{\pi}\int_{-\frac{\pi}{2}}^{\frac{\pi}{2}} F(\theta,\phi)\ \sin\theta\ d\theta\ d\phi \end{bmatrix} \quad (35)$$

where the x-direction is the spacecraft ram direction, the z-direction points towards Earth, and the y-direction completes the right hand rule. Applying this to Envisat, we obtain:

$$\mathbf{D} = \begin{bmatrix} -0.6001 \\ -0.0073 \\ 0.0986 \end{bmatrix} \quad (36)$$

As one can see, the integrated flux is still mostly in the incoming ram direction due to the symmetry of the directional flux. The reduction factor obtained is therefore $\|\mathbf{D}\| = 0.6082$, which, when applied to the sum of the impactor masses from the Monte Carlo simulations yields:

$$\begin{aligned} \sum_j m_j &= 0.6082 \times 3.00 \times 10^{-4}\ \text{kg} \\ &= 1.8246 \times 10^{-4}\ \text{kg} \end{aligned} \quad (37)$$

The above value is very close to the sum of the two impactors computed in Eq. (34) and therefore provides a satisfactory validation of the stochastic model.

6. CONCLUSION

Following the methodology of [14], a framework for including the effect of hypervelocity impacts in the orbit propagation of spacecraft was outlined, making use of a compound Poisson process and transforming the differential equations of motion into stochastic differential equations through the impact fluxes of the MASTER-2009 model. The framework was applied to propagate the orbits of four satellites solely under bombardment of debris and micrometeoroids. The results of the Monte Carlo simulation showed that the effect on the orbital parameters is very small, likely negligible when compared to other orbital disturbances. Two analytical test cases comparing the orbit decay seen in the simulations to a Hohmann transfer orbit from two head-on collisions were also performed and brought additional confidence in the validity of the stochastic model.

ACKNOWLEDGMENTS

This work was supported by Hydro-Québec and the Faculty of Engineering at McGill University through the McGill Engineering Doctoral Award and by the Natural Sciences and Engineering Research Council of Canada (NSERC). Computations were made on the supercomputer Guillimin from McGill University, managed by Calcul Québec and Compute Canada. Its operation is funded by the Canada Foundation for Innovation (CFI), ministère de l'Économie, de la Science et de l'Innovation du Québec (MESI) and the Fonds de recherche du Québec - Nature et technologies (FRQ-NT).

REFERENCES

1. Bastida Virgili B., Lemmens S., Krag H., (2014). Investigation on Envisat attitude motion, e.Deorbit Workshop, The Netherlands.
2. Bate R. R., Mueller D. D., White J. E., (1971). *Fundamentals of astrodynamics*, Courier Corporation.
3. Drolshagen G., (2008). Impact effects from small size meteoroids and space debris, *Adv. Space Res.*, 41, 1123-1131.
4. European Space Agency, (2017). Clean Space, <http://www.esa.int/Our_Activities/Space_Engineering_Technology/Clean_Space/How_many_space_debris_objects_are_currently_in_orbit> (accessed 22.01.2017).
5. Flegel S., Gelhaus J., Möckel M., et al., (2011). Maintenance of the ESA MASTER Model - Final Report, Tech. Rep., ESA Contract Number 21705/08/D/HK, European Space Agency.
6. Hughes P.C., (2004). *Spacecraft Attitude Dynamics*, Dover Publications Inc.
7. Kucharski D., Kirchner G., Koidl F., et al., (2014). Attitude and spin period of space debris Envisat measured by satellite laser ranging, *IEEE Trans. Geosci. Remote Sensing*, 52, 7651-7657.
8. Liou J.-C., Johnson N.L., (2006). Risks in space from orbiting debris, *Science*, 311, 340-341.
9. NASA, (2017). <https://www.nasa.gov/mission_pages/asteroids/overview/fastfacts.html> (accessed 22.01.2017).
10. Pardini C., Tobiska W. K., Anselmo L., (2006). Analysis of the orbital decay of spherical satellites using different solar flux proxies and atmospheric density models, *Adv. Space Res.*, 37, 392-400.
11. Platen E., Bruti-Liberati N., (2010). *Numerical Solution of Stochastic Differential Equations with Jumps in Finance*, Springer-Verlag Berlin Heidelberg.
12. Rival M., Mandeville J.C., (1999). Modeling of ejecta produced upon hypervelocity impacts, *Space Debris*, 1, 45-57.
13. Rubincam, D. P., (1982). On the secular decrease in the semimajor axis of LAGEOS's orbit, *Celest. Mech.*, 26, 361-382.
14. Sagnières L.B.M., Sharf I., (2017). Stochastic modeling of hypervelocity impacts in attitude propagation of space debris, *Adv. Space Res.*, 59, 1128-1143.
15. Schildknecht T., Musci R., Flohrer T., (2008). Properties of the high area- to-mass ratio space debris population at high altitudes, *Adv. Space Res.*, 41, 1039-1045.